HHS Public Access

Author manuscript

J Pediatr Surg. Author manuscript; available in PMC 2020 June 01.

Published in final edited form as:

J Pediatr Surg. 2019 June ; 54(6): 1192–1197. doi:10.1016/j.jpedsurg.2019.02.028.

Down-Regulation of MYCN Protein by CX-5461 Leads to Neuroblastoma Tumor Growth Suppression

Jordan S. Taylor, MD[1], **Jasmine Zeki, BS**[1], **Kimberly Ornell, ME**[2], **Jeannine Coburn, PhD**[2], **Hiroyuki Shimada, MD, PhD**[3], **Naohiko Ikegaki, PhD**[4], and **Bill Chiu, MD**[1,5,†]

[1]Department of Surgery, Stanford University, Stanford, CA

[2]Department of Biomedical Engineering, Worcester Polytechnic Institute, Worcester, MA

[3]Department of Pathology and Laboratory Medicine, Children's Hospital Los Angeles, University of Southern California, Los Angeles, CA

[4]Department of Anatomy and Cell Biology, University of Illinois at Chicago, Chicago, IL

[5]Department of Surgery, University of Illinois at Chicago, Chicago, IL

Abstract

Purpose: MYCN oncogene amplification is an independent predictor of poor prognosis in neuroblastoma. CX-5461 is a small molecular inhibitor that prevents initiation of ribosomal RNA (rRNA) synthesis by RNA Pol I, down-regulating MYCN/MYC proteins. We hypothesize that neuroblastoma tumor growth can be suppressed by CX-5461.

Methods: MYCN-amplified (KELLY, IMR5) and non-amplified (SY5Y, SKNAS) neuroblastoma cells were treated with CX-5461. MYCN/MYC expression after 24–48 hours was determined by Western blot. Orthotopic neuroblastoma tumors created in mice using KELLY cells were treated with CX-5461-loaded silk films implanted locally. Tumor growth was monitored using ultrasound. Histologic evaluation of tumors was performed.

Results: IC_{50} for KELLY, IMR5, SY5Y, and SKNAS cells to CX-5461 was 0.75μM, 0.02μM, 0.8μM, and 1.7μM, respectively. CX-5461 down-regulated MYCN and MYC proteins at 0.25–1.0μM on Western blot analysis. CX-5461-loaded silk film released 23.7±3μg of the drug in 24 hours and 48.2±3.9μg at 120 hours. KELLY tumors treated with CX-5461-loaded film reached $800mm^3$ after 7.8±1.4 days, while those treated with control film reached the same size on 5.1±0.6 days (p=0.03). CX-5461-treated tumors showed collapse of nucleolar hypertrophy and MYCN protein downregulation.

Conclusion: We demonstrated that local delivery of CX-5461 via sustained release platform can suppress orthotopic neuroblastoma tumor growth, especially those with MYCN/MYC overexpression.

[†]**Corresponding Author:** Bill Chiu M.D., Department of Surgery - Pediatric Surgery, Stanford University, 300 Pasteur Drive, Always Building M116, Stanford, CA 94305, Telephone: (650) 723 - 6439, Fax: (650) 725 - 5577, bhsc@stanford.edu.

Keywords

Neuroblastoma; CX-5461; MYCN; MYC; Oncogene; Silk fibroin; Local drug delivery platform

1. INTRODUCTION

Neuroblastoma is one of the most common pediatric solid tumors, accounting for nearly 10% of all pediatric malignancies and 15% of all pediatric oncology deaths.[1, 2] The presentation and clinical course of neuroblastoma is incredibly heterogeneous and varies greatly depending on tumor location and biology. Low- and intermediate-risk disease are often successfully treated with surgical resection alone, with long-term survival rates greater than 90%.[3] Patients with high-risk diseases, however, despite advances in surgical and multimodal non-surgical treatments, have a five-year overall survival rate of 40–50%.[4]

Risk stratification and prognostication for neuroblastoma has been an ongoing area of research. The most recent neuroblastoma classification system was developed by the International Neuroblastoma Risk Group (INRG) and utilizes seven clinical and biological variables.[5, 6] The presence of MYCN oncogene amplification is a key determinant within the INRG system that designates neuroblastoma as high-risk. The MYC family proteins function as transcriptional regulators and are pivotally involved with differentiation, cell growth, and proliferation.[7] The deregulated MYC oncoproteins, however, are known to robustly activate ribosomal RNA (rRNA) synthesis and global protein translation, contributing to tumorigenesis.[8] MYCN amplification is present in 20–25% of neuroblastoma tumors and has long been recognized for its association with advanced disease and poor prognosis.[2, 9, 10] The MYCN oncoprotein is known to contribute to metastatic behavior, evasion of immune surveillance, and blockade of differentiation pathways.[11–15] There is also evidence that MYCN overexpression is associated with angiogenesis and cell proliferation.[16] Separate from MYCN-amplified neuroblastomas, approximately 10% of undifferentiated or poorly differentiated neuroblastomas express high levels of MYC (c-Myc) and are also associated with a poor prognosis, with three-year event free survival around 46%.[17]

Overexpression of MYC family protein (MYCN or MYC) leads to activation of rRNA synthesis by RNA Polymerase I (Pol I), a polyprotein complex that is also widely activated in cancer.[18] CX-5461 is a small molecule inhibitor of Pol I transcription and has been shown to have antitumor activity by inhibiting the initiation stage of rRNA synthesis.[19] We hypothesize that inhibition of MYC family proteins such as MYCN through Pol I inhibition via CX-5461 will lead to decreased neuroblastoma tumor growth. We aim to demonstrate this effect using an orthotopic neuroblastoma xenograft model and sustained release silk fibroin delivery platform. Silk-based delivery platforms offer numerous benefits and have been studied in neuroblastoma tumor xenograft models [20, 21]: they can be formulated to be injectible or implantable, augmented to tailor the drug release profile, are biocompatible and used in surgery. By combining a targeted therapy against MYCN overexpression and a local delivery system that minimizes systemic toxicity, we hope to develop an effective treatment that is readily translatable to clinical care.

2. METHODS

2.1 Silk fibroin extraction

Silk fibroin from *Bombxy mori* silkworm cocoons (Tajima Shoji Co., Yokohama, Japan), kindly provided by Dr. David L. Kaplan at Tufts University, was extracted as previously described.[22] Briefly, five grams of cocoons were cut into approximately one cm^2 pieces and boiled in 0.02 M Na_2CO_3 for 30 minutes to extract the silk fibroin. The extracted silk fibroin fibers were dried overnight, then dissolved in 9.3 M LiBr at 60°C for three hours. The dissolved silk fibroin was dialyzed in 3,500 MWCO dialysis tubing (Fisher Scientific, Hampton, NH) against deionized water for two days with a minimum of six water changes. The aqueous silk fibroin solution was stored at 4°C for future use.

2.2 Silk film fabrication

Silk films were fabricated as previously described.[20, 23, 24] Briefly, 192 μL of 4% (w/v) silk fibroin was pipetted onto 11 cm x 17 cm polydimethylsiloxane (Sylgard®184, Dow Corning, Auburn, MI) and allowed to dry overnight. Seven-millimeter diameter disks were punched from the dried silk films and autoclaved to induce the β-sheet transition, rendering the materials insoluble.

2.3 CX-5461 loading and drug release studies

CX-5461-loaded silk films were formulated via an adsorption from solution method. Silk films (1.12 ± 0.21 mg) were loaded with CX-5461 via adsorption presumably through electrostatic interaction between the positively charge CX-5461 (basic pKa = 9.03; Millipore Sigma, Burlington, MA) and negatively charge silk fibroin (isoelectric points ranging from 4.0 – 5.2).[21] CX-5461 was dissolved in 12 mM glacial acetic acid at 10 mg/mL. Films were submerged in one mL of 200 μg/mL CX-5461 solution (diluted in 20 mM phosphate buffer pH 7.4) for three days. CX-5461 concentration was determined via UV/visible spectroscopy at 344 nm using a standard curve ranging from 1.6 μg/mL to 200 μg/mL. The CX-5461 loading was calculated as follows:

$$\left(Initial\ concentraction\left(\frac{\mu g}{mL}\right) - Final\ concentraction\left(\frac{\mu g}{mL}\right)\right) * 1\ mL = Mass\ Loaded\ (\mu g)$$

For drug release studies, CX-5461-loaded silk films with 105 μg of the drug were placed into one mL phosphate buffered saline (PBS, pH 7.4) at 37°C. The UV absorbance was read at each time point and the solution replaced into the sample tube for study continuation.

2.4 Cell culture and determination of half maximal inhibitory concentration (IC_{50})

MYCN-amplified human neuroblastoma cell lines (KELLY, IMR5) and non-MYCN-amplified cell lines (SY5Y, SKNAS) were used in this study. Of note, the non-MYCN-amplified cell lines express high levels of MYC (c-Myc) protein. Both MYCN and MYC proteins belong to the MYC family proteins. KELLY cells were purchased from Sigma-Aldrich (St Louis, MO); IMR5 cells were a gift of Roger H. Kennett (University of Pennsylvania, PA. USA); SY5Y and SKNAS cell lines were obtained from American Type Culture Collection (ATCC, Manassas, VA). All cell lines were maintained in RPMI 1640

(HyClone, Logan, UT) supplemented with 5% fetal bovine serum, 1% OPI, 1% a,l-glutamine, and 250 μL gentamycin. All cells were maintained in a 5% CO_2 atmosphere at 37°C and passaged via trypsinization when they reached 80% confluence. In order to determine the half maximal inhibitory concentration (IC_{50}) of CX-5461, all cell lines were exposed to varying doses of CX-5461 for two days. The IC_{50} was defined as the amount of drug required to kill 50% of the cells.

2.5 Western blot

Western blot analysis was performed after cell lines were treated with varying concentrations of CX-5461, as previously described.[25, 26] Analysis was performed using anti-pan-MYC antibody (NCMII 143) and the anti-ß-actin antibody (Santa Cruz) to ascertain equal protein loading.[27] Band intensities were quantified with ImageJ software (National Institutes of Health, http://rsb.info.nih.gov/ij/), normalizing MYCN/MYC to ß-actin. Intensities of the treatment groups were compared to the control groups for each cell line using Student's t test, with p values <0.05 considered significant.

2.6 Mouse orthotopic neuroblastoma model and ultrasound monitoring

All animal procedures were performed in accordance with NIH protocols on Humane Care and Use of Laboratory Animals and approved by the Institutional Animal Care and Use Committee of University of Illinois at Chicago. Orthotopic neuroblastoma xenografts were established in seven-week old female NCr nude mice (Harlan, Indianapolis, IN, USA), as previously described.[20] In brief, an incision was made over the left flank and the left adrenal gland was injected with 10^6 KELLY cells in two μL PBS. Closure was completed in two layers. Tumor volume was serially measured with high frequency ultrasound using a VisualSonics Vevo 2100 sonographic probe (Toronto, Ontario, Canada) as previously described.[28]

2.7 Implantation of silk film into tumor

Once tumor size reached 100 mm^3, the mice were briefly anesthetized as described above. The previous incision was re-opened to gain direct access to the orthotopic tumor. A small incision was made through the capsule of the tumor using electrocautery, and the CX-5461-loaded silk film or the unloaded control film was implanted into the center of the tumor. The mice were closed in a similar fashion and tumor volumes were followed with serial ultrasound.

2.8 Immunohistochemistry

Animals were monitored until tumor volume exceeded 1000 mm^3, at which point the animals were sacrificed and tumors were harvested and preserved in 10% buffered formalin. Tumor specimens were embedded in paraffin and sectioned for immunohistochemical staining and hematoxylin and eosin (H&E). The anti-MYCN mouse monoclonal antibody (NCM II 100) was used for immunohistochemistry as previously described.[7, 27]

2.9 Statistical analysis

Tumor sizes and post-operative days were entered into a scatter plot, and a best fit curve with an associated equation was created for each animal. Tumor size (500 mm^3, 600 mm^3, 700 mm^3, or 800 mm^3) was calculated from these equations as previously described.[28] In brief, we solved for the post-operative day using the "goal seek" function under the "what-if analysis" (Microsoft Excel, 2011, version 14.7.4, Redmond, Washington). The post-operative days obtained for each given tumor size were compared using Student's t test, with p values <0.05 considered statistically significant.

3. RESULTS

3.1 CX-5461 drug release

The loading and release of CX-5461 from silk fibroin films was evaluated *in vitro* (Figure 1). Silk fibroin films were loaded with 105.1 ± 15 μg of CX-5461. A burst release of 28.9 ± 7.5 μg (27.5 ± 8.5 %) was observed after the first 24 hours. A linear release was observed from days six to 18 with an average release of 3.1 μg/day (3% per day) of CX-5461 and an R^2 value of 0.99. Full release of CX-5461 was achieved in 21 days.

3.2 IC_{50} determination and protein expression analysis

KELLY, IMR5, SY5Y, and SKNAS cells exposed to varying concentrations of CX-5461 for two days demonstrated a dose-dependent cell death (Figure 2A). IC_{50} for these cell lines was 0.75μM, 0.02μM, 0.8μM, and 1.7μM, respectively. The Western blot analysis demonstrated down-regulation of MYCN protein in the CX-5461-treated IMR5 cells starting at the 24-hour time point compared to untreated cells, and decreased expression in the KELLY cells after 48 hours relative to control ($p = 0.005$ and $p = 0.006$, respectively; Figure 2B). There was also significant decrease in MYC expression in CX-5461-treated SY5Y and SKNAS cell lines at both time points (24- and 48-hour) compared to untreated cells ($p = 0.01$ and $p = 0.014$, respectively).

3.3 Orthotopic tumor growth following CX-5461 compared to control

Neuroblastoma tumors implanted with CX-5461-loaded silk film demonstrated decreased tumor growth compared to tumors treated with blank control film ($p < 0.05$). CX-5461 treated tumors reached 500 mm^3 in 5.0 ± 0.7 days vs 2.4 ± 1.3 days for control ($p = 0.02$). Similarly, CX-5461 treated tumors reached 600 mm^3 in 6.0 ± 0.9 days vs 3.3 ± 1.1 days for control ($p = 0.02$); reached 700 mm^3 in 6.9 ± 1.2 days vs 4.2 ± 0.9 days for control ($p = 0.02$); and 800 mm^3 in 7.8 ± 1.4 days vs 5.2 ± 0.6 days for control ($p = 0.03$), respectively (Figure 3).

3.4 Histology

H&E staining showed that the control tumors were composed of neuroblasts characterized by nucleolar hypertrophy (presence of one to a few prominent nucleoli), indicative of aumented rRNA synthesis (Figure 4). Neuroblasts in the CX-5461-treated tumors, however, had conventional salt-and-pepper nuclei without nuclear hypertrophy. Immunohistochemical examination further demonstrated high expression of MYCN protein in the nuclei of control

tumors. In contrast, CX-5461-treated tumors demonstrated markedly reduced staining for MYCN protein. These observations support that RNA Pol I inhibition by the drug resulted in collapse of enlarged nucleoli (the location of rRNA synthesis) and subsequent downregulation of MYCN protein expression.

4. DISCUSSION

We were able to demonstrate the growth inhibition effects of CX-5461, a small molecular inhibitor of Pol I in both MYCN-amplified and non-amplified neuroblastoma tumor cells. The effect is dose dependent and involves the down-regulation off MYCN and MYC proteins. Using a MYCN-amplified cell line, we created an orthotopic neuroblastoma murine model to preclinically study CX-5461 activity, combining this targeted therapy with local drug delivery strategies. CX-5461 delivered locally in a sustained release fashion significantly suppressed neuroblastoma tumor growth compared to control tumors. Moreover, CX-5461 markedly reduced the size of nucleoli, the location of rRNA synthesis and downregulated MYCN expression.

Targeting MYCN activity is emerging as a promising adjunctive therapy for high-risk malignancies. Kang et al. was able to induce apoptosis and cell differentiation in MYCN-amplified cells by using small interfering RNA (siRNA) as a directed treatment against MYCN overexpression.[29] Niemas-Teshiba et al. has recently demonstrated the antitumor effects of Halofuginone, an aminoacyl tRNA synthetase, which similarly down-regulates MYCN/MYC protein synthesis.[7] Burkhart et al. examined the use of antisense oligonucleotides to inhibit MYCN expression *in vitro* and in murine model of neuroblastoma.[30] However, these methods are not without various challenges. Oligonucleotides, as an example, are rapidly degraded by nucleases, which may limit their clinical utility.

Our model combines a precise anticancer therapy with a local drug delivery platform, which could significantly reduce the side effect profile and improve local tumor control. CX-5461 has been shown to have a low oral bioavailability (24%) in mice and is difficult to maintain in solution.[31] Intravenous CX-5461 needs to be solubilized in pH 3.5, which negatively affects pharmacokinetics and biodistribution, leading Leung et al. to develop a conjugated liposomal formation.[32] Our method, however, ensures complete bioavailability directly to the tumor bed, which can significantly reduce systemic toxicity.[20]

Pre-clinical and Phase I clinical trials (ACTRN12613001061729) have shown that CX-5461 is well tolerated with minimal adverse events.[33, 34] Though previous trials of CX-5461 have been conducted in patients with advanced hematologic malignancies, there are ongoing Phase I/II clinical studies of CX-5461 infusions in patients with advanced staged BRCA-deficient breast cancers (NCT02719977, https://clinicaltrials.gov/ct2/show/NCT02719977?term=CX-5461&rank=1). To date, the trials have found that CX-5461 is well tolerated with minimal side effects (reversible and preventable photosensitivity).[35] Future clinical trials will have to explore the feasibility and efficacy of using locally distributed CX-5461 for improved local control in patients with advanced staged neuroblastoma.

The benefits of local anti-tumor therapy have been studied in neuroblastoma tumor models and have several potential clinical uses.[36] Advanced staged neuroblastoma is often treated with neoadjuvant therapy, which could provide an opportunity for local treatment with an implantable delivery system loaded with CX-5461 or other anti-tumor therapy.[20] Minimally invasive techniques such as image guided injections could be adapted to deliver injectible anti-tumor therapy, providing additional benefits.[28] Alternatively, there is an opportunity for local delivery of anti-tumor therapy in a sustained release platform at the time of surgery to improve local control, particularly in the case of an incomplete resection. Previous studies have shown improved local control when local anti-tumor therapy is used in combination with a partial resection of neuroblastoma.[23]

While this work demonstrates that CX-5461 can inhibit neuroblastoma tumor growth, more work is needed to fully understand the mechanism of inhibition. We hypothesize that CX-5461 causes a global decrease in MYC family protein expression as a result of decreased rRNA synthesis, though more studies are needed to confirm the therapeutic benefit. The study is limited by the fact that only one MYCN-amplified cell line (KELLY) was used to create a xenograft model. Future work using other MYCN-amplified or MYC-overexpressed in vivo models might help to explain the mechanism of inhibition or demonstrate a variable response to CX-5461.

ACKNOWLEDGEMENTS

This work was supported by the National Institutes of Health grants R01NS094218 (B.C.).

6. REFERENCES

[1]. Maris JM, Hogarty MD, Bagatell R, Cohn SL. Neuroblastoma. Lancet 2007;369(9579):2106–20. [PubMed: 17586306]

[2]. Pizzo PA, Poplack DG. Principles and practice of pediatric oncology. Seventh ed.: Lippincott Williams & Wilkins; 2015.

[3]. De Bernardi B, Mosseri V, Rubie H, Castel V, Foot A, Ladenstein R, et al. Treatment of localised resectable neuroblastoma. Results of the LNESG1 study by the SIOP Europe Neuroblastoma Group. Br J Cancer 2008;99(7):1027. [PubMed: 18766186]

[4]. Whittle SB, Smith V, Doherty E, Zhao S, McCarty S, Zage PE. Overview and recent advances in the treatment of neuroblastoma. Expert Rev Anticancer Ther 2017;17(4):369–86. [PubMed: 28142287]

[5]. Cohn SL, Pearson AD, London WB, Monclair T, Ambros PF, Brodeur GM, et al. The International Neuroblastoma Risk Group (INRG) classification system: an INRG task force report. J Clin Oncol 2009;27(2):289. [PubMed: 19047291]

[6]. Monclair T, Brodeur GM, Ambros PF, Brisse HJ, Cecchetto G, Holmes K, et al. The International Neuroblastoma Risk Group (INRG) staging system: an INRG task force report. J Clin Oncol 2009;27(2):298. [PubMed: 19047290]

[7]. Niemas-Teshiba R, Matsuno R, Wang LL, Tang XX, Chiu B, Zeki J, et al. MYC-family protein overexpression and prominent nucleolar formation represent prognostic indicators and potential therapeutic targets for aggressive high-MKI neuroblastomas: a report from the children's oncology group. Oncotarget 2018;9(5):6416. [PubMed: 29464082]

[8]. Dang CV. MYC, metabolism, cell growth, and tumorigenesis. Cold Spring Harb Perspect Med 2013;3(8):a014217. [PubMed: 23906881]

[9]. Brodeur GM, Seeger RC, Schwab M, Varmus HE, Bishop JM. Amplification of N-myc in untreated human neuroblastomas correlates with advanced disease stage. Science 1984;224(4653):1121–4. [PubMed: 6719137]

[10]. Seeger RC, Brodeur GM, Sather H, Dalton A, Siegel SE, Wong KY, et al. Association of multiple copies of the N-myc oncogene with rapid progression of neuroblastomas. N Engl J Med 1985;313(18):1111–6. [PubMed: 4047115]

[11]. Zaizen Y, Taniguchi Si, Noguchi Si, Suita S. The effect of N-myc amplification and expression on invasiveness of neuroblastoma cells. J Pediatr Surg 1993;28(6):766–9. [PubMed: 8331499]

[12]. Benard J Genetic alterations associated with metastatic dissemination and chemoresistance in neuroblastoma. Eur J Cancer 1995;31(4):560–4.

[13]. Goodman LA, Liu BC, Thiele CJ, Schmidt ML, Cohn SL, Yamashiro JM, et al. Modulation of N-myc expression alters the invasiveness of neuroblastoma. Clin Exp Metastasis 1997;15(2):130–9. [PubMed: 9062389]

[14]. Cotterman R, Knoepfler PS. N-Myc regulates expression of pluripotency genes in neuroblastoma including lif, klf2, klf4, and lin28b. PloS One 2009;4(6):e5799. [PubMed: 19495417]

[15]. Ben-Yosef T, Yanuka O, Halle D, Benvenisty N. Involvement of Myc targets in c-myc and N-myc induced human tumors. Oncogene 1998;17(2):165. [PubMed: 9674700]

[16]. Huang M, Weiss WA. Neuroblastoma and MYCN. Cold Spring Harb Perspect Med 2013;3(10):a014415. [PubMed: 24086065]

[17]. Wang L, Teshiba R, Ikegaki N, Tang X, Naranjo A, London W, et al. Augmented expression of MYC and/or MYCN protein defines highly aggressive MYC-driven neuroblastoma: a Children's Oncology Group study. British journal of cancer 2015;113(1):57. [PubMed: 26035700]

[18]. Grandori C, Gomez-Roman N, Felton-Edkins ZA, Ngouenet C, Galloway DA, Eisenman RN, et al. c-Myc binds to human ribosomal DNA and stimulates transcription of rRNA genes by RNA polymerase I. Nature cell biology 2005;7(3):311. [PubMed: 15723054]

[19]. Drygin D, Lin A, Bliesath J, Ho C, O'Brien S, Proffitt C, et al. Targeting RNA polymerase I with an oral small molecule CX-5461 inhibits ribosomal RNA synthesis and solid tumor growth. Cancer Res 2010:canres. 1728.2010.

[20]. Coburn J, Harris J, Zakharov AD, Poirier J, Ikegaki N, Kajdacsy-Balla A, et al. Implantable chemotherapy-loaded silk protein materials for neuroblastoma treatment. Int J Cancer 2017;140(3):726–35. [PubMed: 27770551]

[21]. Coburn JM, Na E, Kaplan DL. Modulation of vincristine and doxorubicin binding and release from silk films. J Control Release 2015;220:229–38. [PubMed: 26500149]

[22]. Rockwood DN, Preda RC, Yücel T, Wang X, Lovett ML, Kaplan DL. Materials fabrication from Bombyx mori silk fibroin. Nat Protoc 2011;6(10):1612–31. [PubMed: 21959241]

[23]. Chiu B, Coburn J, Pilichowska M, Holcroft C, Seib FP, Charest A, et al. Surgery combined with controlled-release doxorubicin silk films as a treatment strategy in an orthotopic neuroblastoma mouse model. Br J Cancer 2014;111(4):708–15. [PubMed: 24921912]

[24]. Seib FP, Coburn J, Konrad I, Klebanov N, Jones GT, Blackwood B, et al. Focal therapy of neuroblastoma using silk films to deliver kinase and chemotherapeutic agents in vivo. Acta Biomater 2015;20:32–8. [PubMed: 25861948]

[25]. Torres J, Regan PL, Edo R, Leonhardt P, Jeng EI, Rappaport EF, et al. Biological effects of induced MYCN hyper-expression in MYCN-amplified neuroblastomas. Int J Oncol 2010;37(4): 983–91. [PubMed: 20811720]

[26]. Regan PL, Jacobs J, Wang G, Torres J, Edo R, Friedmann J, et al. Hsp90 inhibition increases p53 expression and destabilizes MYCN and MYC in neuroblastoma. Int J Oncol 2011;38(1):105–12. [PubMed: 21109931]

[27]. Ikegaki N, Bukovsky J, Kennett RH. Identification and characterization of the NMYC gene product in human neuroblastoma cells by monoclonal antibodies with defined specificities. Proc Natl Acad Sci U S A 1986;83(16):5929–33. [PubMed: 2426708]

[28]. Zeki J, Taylor JS, Yavuz B, Coburn J, Ikegaki N, Kaplan DL, et al. Disseminated injection of vincristine-loaded silk gel improves the suppression of neuroblastoma tumor growth. Surg 2018;164(4):909–15.

[29]. Kang J-H, Rychahou PG, Ishola TA, Qiao J, Evers BM, Chung DH. MYCN silencing induces differentiation and apoptosis in human neuroblastoma cells. Biochem Biophys Res Commun 2006;351(1):192–7. [PubMed: 17055458]

[30]. Burkhart CA, Cheng AJ, Madafiglio J, Kavallaris M, Mili M, Marshall GM, et al. Effects of MYCN antisense oligonucleotide administration on tumorigenesis in a murine model of neuroblastoma. J Natl Cancer Inst 2003;95(18):1394–403. [PubMed: 13130115]

[31]. Haddach M, Schwaebe MK, Michaux J, Nagasawa J, O'Brien SE, Whitten JP, et al. Discovery of CX-5461, the first direct and selective inhibitor of RNA polymerase I, for cancer therapeutics. ACS Med Chem Lett 2012;3(7):602–6. [PubMed: 24900516]

[32]. Leung AW, Anantha M, Dragowska WH, Wehbe M, Bally MB. Copper-CX-5461: A novel liposomal formulation for a small molecule rRNA synthesis inhibitor. J Control Release 2018;286:1–9. [PubMed: 30016731]

[33]. Harrison SJ, Khot A, Brajanovski N, Cameron D, Hein N, McArthur GA, et al. A phase 1, open-label, dose escalation, safety, PK and PD study of a first in class Pol1 inhibitor (CX-5461) in patients with advanced hematologic malignancies (HM). Proceedings of the 2015 American Society of Clinical Oncology Annual Meeting Chicago, IL, USA; 5 2, 2015.

[34]. Hein N, O'Brien S, Drygin D, Harrison SJ, Khot A, Cullinane C, et al. Inhibition of RNA Polymerase I transcription by CX-5461 as a therapeutic strategy for the cancer-specific activation of p53 in highly refractory haematological malignancies. Blood 2013;122(21):3941.

[35]. Hilton J, Cescon DW, Bedard P, Ritter H, Tu D, Soong J, et al. 44OCCTG IND.231: A phase 1 trial evaluating CX-5461 in patients with advanced solid tumors. Ann Oncol 2018;29(suppl_3):mdy048.03-mdy.03.

[36]. Harris J,C Klonoski S, Chiu B. Clinical considerations of focal drug delivery in cancer treatment. Current drug delivery 2017;14(5):588–96. [PubMed: 28240175]

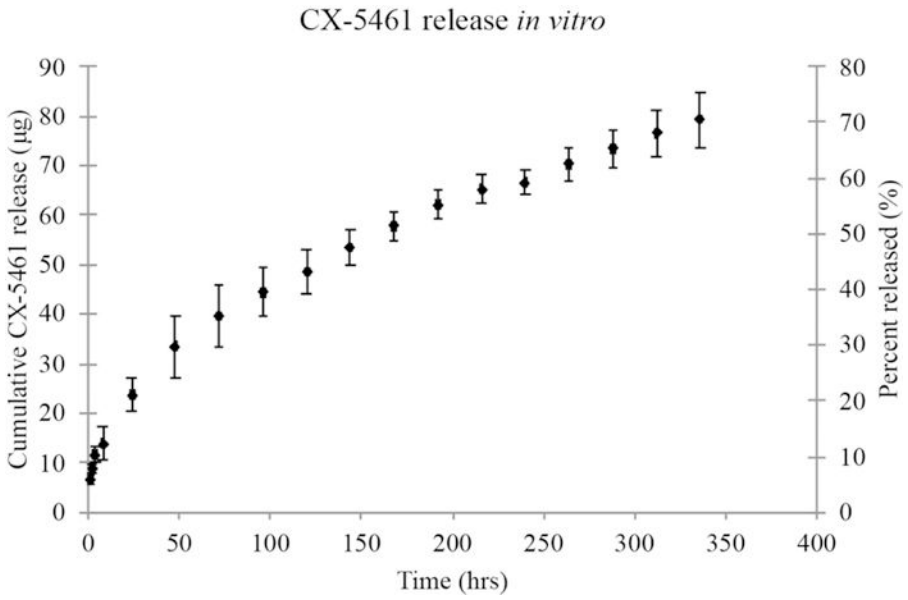

Figure 1.

Amount (µg) of CX-5461 released from silk films that were loaded with 105 µg CX-5461 and placed in PBS. Error bars indicate standard deviation in µg.

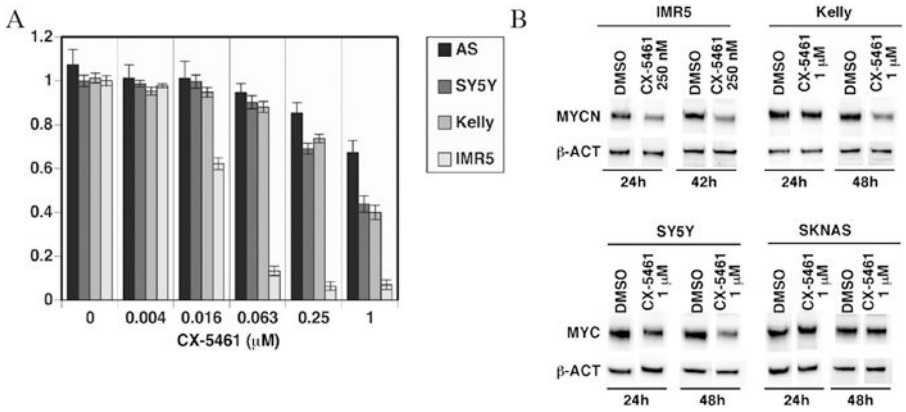

Figure 2.

(A) IC_{50} of CX-5461 in KELLY, IMR5, SY5Y, and SKNAS cells, displayed as portion of viable cells after 24 – 48 hrs. (B) Representative images of Western blot analysis of MYCN/MYC expression in KELLY, IMR5, SY5Y and SKNAS cell lines after CX-5461 treatment.

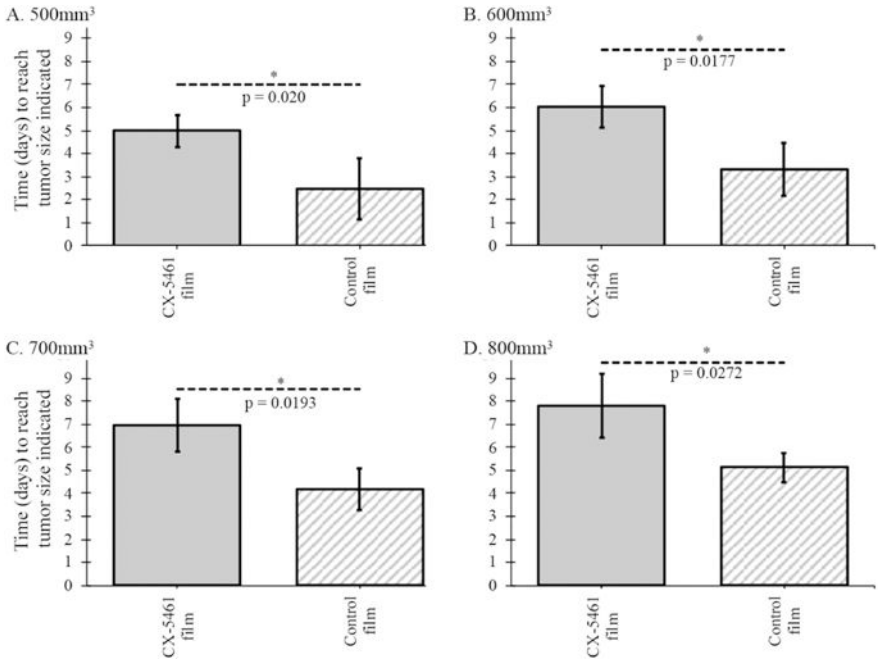

Figure 3.

Growth pattern for orthotopic neuroblastoma tumors treated with CX-5461-loaded silk film compared to tumors treated with blank silk film. Time (days) for tumor to reach (A) 500 mm^3, (B) 600 mm^3, (C) 700 mm^3, and (D) 800 mm^3.

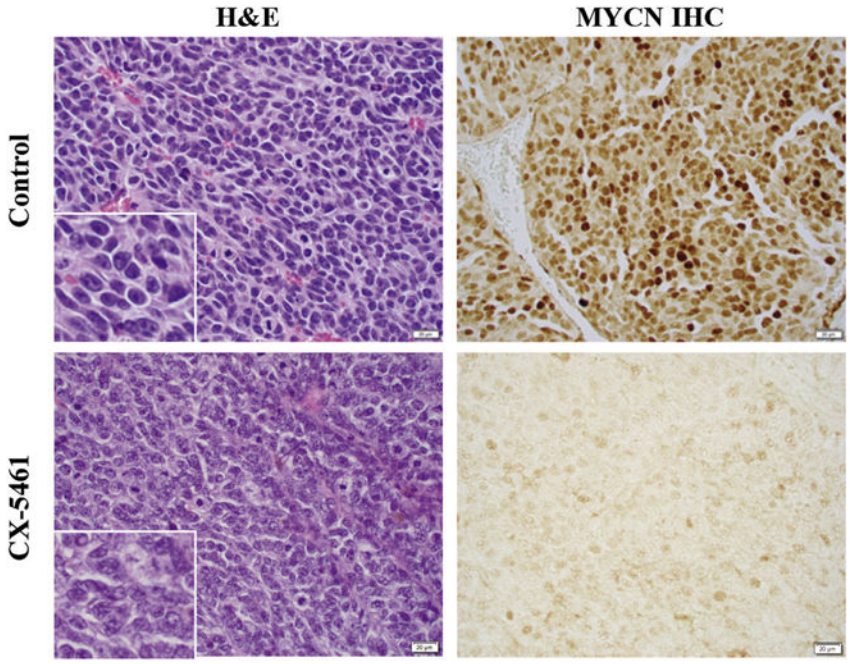

Figure 4.

H&E staining and MYCN expression by immunohistochemistry of tumors treated with CX-5461 or control silk film. The magnification for the main images and inserts was 400X and 1000X, respectively.